First-principles Study on the Properties of CaO(100) Surface Adsorbing Carbon Dioxide①

LI Ming-Yang[a] LI Jia-Yu[b] WU Miao-Miao[a②] WANG Xiao-Lin[c]

[a] (*Department of Materials Science and Engineering, China University of Mining and Technology* (*Beijing*), *Beijing* 100083, *China*)

[b] (*Center on Nanoenergy Research, Guangxi Key Laboratory of Processing for Nonferous Metal and Featured Materials, Guangxi Key Laboratory for Relativity Astrophysics, School of Physical Science & Technology, Guangxi University, Nanning* 530004, *China*)

[c] (*Institute of Nuclear and New Energy Technology, Tsinghua University, Beijing* 100084, *China*)

ABSTRACT The increasing carbon dioxide emissions have a huge impact on the global environment. Carbonation reaction of CaO is regarded as a potential method to capture carbon dioxide. The density functional theory calculations have been performed to investigate the adsorption of CO_2 on CaO(100) surface. This paper systematically studied the adsorption of CO_2 at different adsorption sites on CaO(100) surface and the influence of adsorption angle on adsorption energy. Based on the studying of adsorption sites, adsorption energy and electronic structure of the CO_2/CaO(100) systems, chemical adsorption mainly happens when CO_2 molecules are absorbed on the CaO(100) surfaces, but physical adsorption may also happen. The research found that CO_2 molecules reacted with surface O atom through C, forming monodentate surface carbonate species and tridentate carbonate. Among them, low-coordinated monodentate ligands have a higher stability than tridentate ligands due to the shorter C–O_S bond length of monodentate ligands.

Keywords: density functional theory, CO_2 adsorption, surface chemistry, CaO(100) surface, mono-dentate ligands; DOI: 10.14102/j.cnki.0254–5861.2011–3072

1 INTRODUCTION

CO_2 can be converted into organic matter such as starch by photosynthesis of plants in nature. In the current respect, CO_2 can be used as a carbon resource. How to make CO_2 become an effective carbon resource and how to achieve the capture and reuse of CO_2 remain a research hotspot currently[1-3]. In recent years, facing the global energy crisis and the dramatic increasing carbon dioxide emissions, scientists urgently need to further study how to recycle CO_2[4-13].

Nobel laureate Josef Michl published a commentary article in Nature Chemistry, pointing to the direction of CO_2 photochemical reduction[4]. Ekambaram Balaraman et al. reported on the process of CO_2 catalyzed by noble metals so as to obtain methanol[5]. In the same year, Robert D. Richrdon et al. used an organic amine as a catalyst to photo catalyze the conversion of CO_2 to formic acid[6]. Related research results are published in Nature Chemistry. Additionally, researchers also reported articles on the conversion of CO_2 to methane, carbon monoxide, propanol, and oxalic acid[7-13].

Whether it is the previous Carbon Capture and Sequestration (CCS) or Carbon Capture and Recycling (CCR) technology, the economic capture and

Received 21 December 2020; accepted 6 April 2021

① This research was supported by the National Key Research and Development Program of China (2017YFB0601904), National Natural Science Foundation of China (11404395), and The Fundamental Research Funds for the Central Universities (2013QJ01)

② Corresponding author. Wu Miao-Miao. E-mail: miaomwu@cumtb.edu.cn

separation of carbon dioxide are important links[3, 10-13]. Scholars in various countries are generally consistent with that CO_2 is a relatively weak Lewis acid and can be easily adsorbed on a slightly alkaline surface. Calcium oxide possesses advantages of high adsorption capacity, low cost, and strong practicality (Fig. 1).

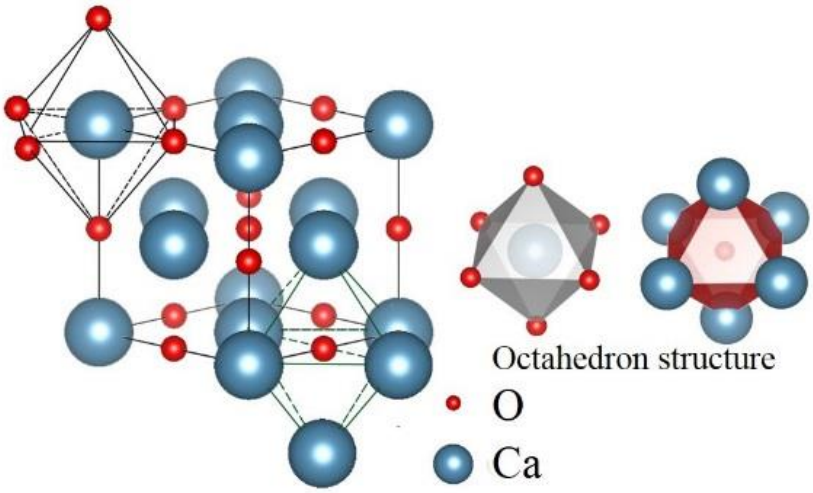

Fig. 1. Crystal structure of CaO

Regardless of the above advantages of CaO in previous articles, it also has the following defects: 1) Slow adsorption rate. Anthony et al. showed that the CO_2 absorption efficiency of CaO gradually decreases with the increase of cycles[14]; 2) Poor cycling stability. Bouquet et al. found that CaO particles are prone to sintering and structurally collapsing at high temperature. $CaCO_3$ generated by carbonation adheres to the surface of the adsorbent, thereby decreasing the pore size and surface area of CaO. As the adsorption progresses, $CaCO_3$ covers the surface of CaO to prevent CaO from further entering the internal adsorbent for reaction, thus resulting in a sharp drop in CaO adsorption capacity and adsorption rate[15].

Numerous works on improving CaO adsorption capacity and cycling stability through methods such as dope, load, support, immobilization of inert/active components, and solvent modification are published[16-23]. Zhao et al. studied the adsorption characteristics of CO_2 on the surface of Ni/CaO by DFT simulation. It is proved that CaO doped with Ni caused a change in the electronic structure of the O_{surf} atom and the 10 wt/% Ni/CaO catalyst is conductive to *in situ* CO_2 capture in biomass pyrolysis[24]. Sun et al. focus on the doped effects of alkali metals, such as Li, Na, K, Rb and Cs, on the uptake of CO_2 and SO_2 by CaO. Adsorption energy calculations indicate that doping Cs on CaO leads to stronger interactions between the adsorbate and the surface due to the structural defects and impurities caused by doping, which affects the stability of CO_2[25]. Although great progress has been made in this filed, there is a few literatures about the role of CO_2 and CaO (100) surfaces.

Pacchioni et al embed the appropriate Madelung field in the model by constructing a cluster model to calculate the adsorption of CO_2 and SO_2 molecules on the surfaces of MgO and CaO[16]. According to the results, two molecules form a weakly bound surface complex on the surface of MgO, and a strongly acting carbonate species is also formed on the surface of CaO. The reason for the above results refers to that the potential energy in CaO is smaller than that of MgO, resulting in more electron delocalization around the O ion, which can effectively overlap with the orbitals of adsorbed molecules. Elly J.Karlsen employed a similar model to analyze the adsorption of CO_2 on alkaline earth metal oxides[17]. When the alkalinity of alkaline earth metal oxides increases, the

tendency for carbonates to form on the surface becomes more apparent. For CaO～BaO, CO_2 is distorted to some extent with the C–O bond distance stretched by up to 0.08 Å and the O–C–O angle reduced down to 130.0°, which is close to the ideal carbonate angle of 120°. The adsorption energy is steadily rising in the series MgO < CaO < SrO < BaO. In addition, the calculated result is consistent with that of Pacchioni[18].

Jensen et al. compare CO_2 adsorption at terrace and defect sites on the (100) face of CaO[19]. The terrace and defect (step and corner) of CaO (100) correspond to five-, four-, and three-coordinated-O^{2-}, respectively. When the O^{2-} coordination number decreases, the Madelung potential decreases, making it easier for electrons to flow from the CaO surface to CO_2. Kadossov et al. proposed that CO_2 bonds to the CaO surface O atoms through C atoms, which is the most stable structure of CO_2 adsorbed on the surface of CaO[20]. CO_2 molecule does not adsorb to the surface through O atoms, which does not react with Ca site. Voigts et al. investigated the adsorption of CO_2 on CaO films by employing Electron Spectroscopy (MIES), Ultraviolet Photoelectron Spectroscopy (UPS), and X-ray Photoelectron Spectroscopy (XPS)[21]. The CO_2 molecule bombards the surface of calcium oxide to form carbonate species. After adsorption, CO_2 will not decompose until the surface of calcium oxide is covered with carbonate. Additionally, the reaction between carbon dioxide and the surface will also stop. R. Besson investigated the interaction effect between CO_2 and CaO surface, and gave calcite in the CaO surface to form nucleation mechanism[22]. Zhang Ying et al. argued that when CO_2 adsorbs the point defect of CaO, an oxygen atom of CO_2 occupies the defect position. At this time, the surface of the substrate is restored to a complete surface, and the CO_2 molecule is decomposed into CO[23].

Recently, above content briefly introduced the related research on carbon dioxide adsorption on the surface of calcium oxide. These studies were based on the adsorption of carbon dioxide on the oxygen active site of CaO. However, there are no published articles on the bridge, hollow, and Ca adsorption of calcium dioxide on the surface of calcium oxide. The adsorption mechanism of metal oxides studied by the first principles study proves that CO_2 tends to maintain linear adsorption on most oxides such as TiO, CrO, VO and MnO[24]. Based on the previous researches, we used the first principles study calculation based on density functional theory by referring to the relevant parameter settings. We presented the adsorption of O-top, bridge, hollow, and Ca-top on the surface of CaO (100) in both the parallel and perpendicular states of carbon dioxide molecules. In the present study, we used charge density, difference charge density, density of states (DOS), and Bader charge analysis methods to characterize the bonding of the adsorbed molecules to the surface. In addition, we also discussed the influence of carbon dioxide surface on the adsorption energy and the bonding due to the different angles and distances.

2 COMPUTATIONAL METHODOLOGY

The calculations of this study are based on DFT and are carried out with the Vienna Ab Initio Simulation Package (VASP)[27]. The interaction between the ions and the valence electrons is described by the projector augmented wave (PAW) method and exchange and correlation treating within the PBE generalized gradient approximation (GGA)[28-30]. A Monkhorst-Pack mesh of 3 × 3 × 1 k-points was used to sample the Brillouin zone for determining the optimized adsorbate structures of CO_2 molecule on the model surfaces, which was increased to 4 × 4 × 1 for the electronic property calculations. The plane wave cutoff energy was 400 eV. All atoms were relaxed until forces are < 0.05 eV/Å and the convergence criteria for the electronic self-consistent loops is set to 1×10^{-6} eV[31-34].

The CaO cubic bulk lattice constant is computed to be 4.812 Å, in good agreement with the experiments (4.81 Å)[35]. A 2 × 2 supercell of the CaO (100) surface with five-layer thick was considered, involving 56 atoms corresponding to five CaO planes. The vacuum region between the slabs was set to 15 Å to avoid interactions between atoms in neighboring cells[36]. Depending on the CO_2 coverage, the coverage corresponds to 1/9. Therefore, we conclude that Van der Waals between adsorbed molecules can

be ignored[37].

During structure optimization, all atoms in the CaO film and the four topmost layers were allowed to relax, while the remaining one layer was frozen at the bulk positions. VESTA 3 software was used to visualize all molecular structures[38]. The five-layer CaO(100) slab model is shown in Fig. 2a, and four different adsorption sites on the substrate are considered, as depicted in Fig. 2b. They are hollow, bridge, Ca-top and O-top sites, respectively.

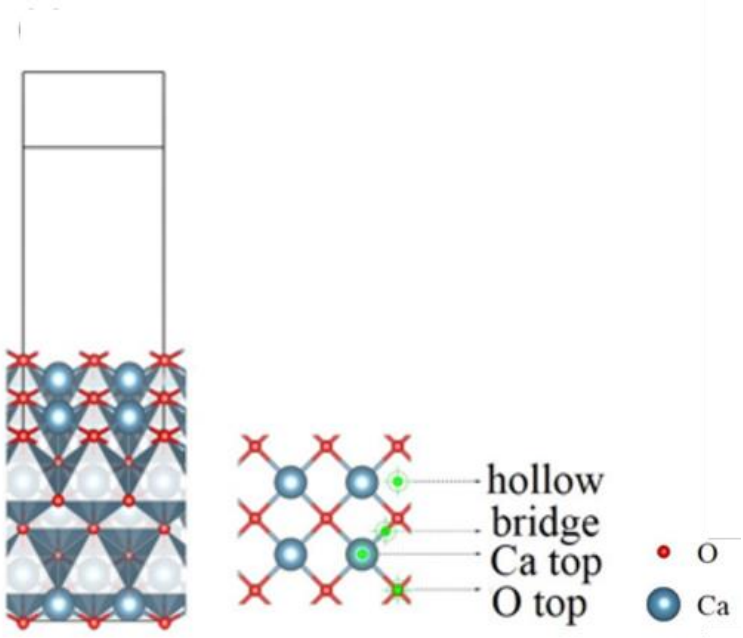

(a) **(b)**

Fig. 2. (a) Five-layer CaO slab model; (b) Top view of the CaO(100) substrate, where the different points include top, bridge, and hollow sites. Red balls represent O atoms and gray balls are Ca atoms

The adsorption energy of CO_2 on the CaO surfaces is calculated as follows:

$$E_a = E_{surf+CO2} - (E_{CO2} + E_{surf}) \quad (1)$$

where E_{surf} represents the energy of clear surface, E_{CO2} is the total energy of the optimized gas phase CO_2 molecule, and $E_{surf+CO2}$ denotes the energy of the whole system.

3 RESULTS and DISCUSSION

3. 1 CO_2 adsorbed on the CaO(100) surface vertically

We calculate the stability of the ordered atomic planes (100), (110) and (111) surfaces of CaO. The atom bonding conditions were analyzed by surface energy, density of states, work function, and charge density. The results showed that (100) surface is more stable than other surfaces because of the Ca–O strong interaction of electron clouds, in agreement with the previous calculations[39, 40]. It provided theoretical guidance for understanding the properties of CaO surface and the adsorption mechanism of CO_2 on the CaO surface. The calculated are listed in Figs. S1～S4.

We have systematically discussed the adsorption of CO_2 molecules on the surface of CaO(100) in a vertical state. As shown in Fig. 3a, b, c, and d, the initial modelling structures of CO_2 are adsorbed vertically on the CaO surface O-top, Ca-top, hollow and bridge. Fig. 3e, f, g and h are the optimized structures calculated by the initial models a, b, c, and d, respectively. Table 2 shows the geometrical properties, adsorption energy, and the vertical height of carbon dioxide from the surface for different adsorption sites for CO_2 adsorption on the CaO(100) surface.

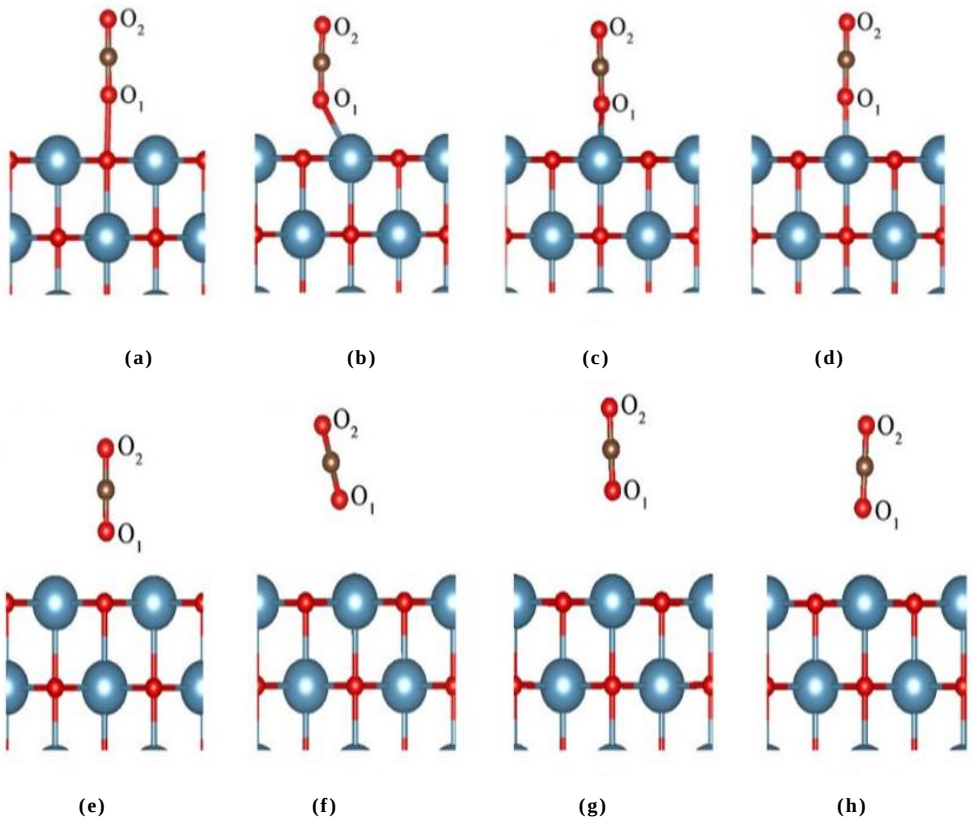

Fig. 3. Adsorption configurations of upright CO_2 on the CaO (100) surface; (a-d) Side views of CO_2 adsorption on the different points of the CaO (100) substrate, O-top, bridge, hollow and Ca-top, respectively; (e-f) Side view of the relaxed structures

Table 1. Adsorption Properties of Upright CO_2 on the CaO (100) Surface

Configuration	d(C–O) (Å)	d(O–O_s) (Å)	∠OCO (°)	H (Å)	E_a (eV)
O-top	1.178	3.269	179.9	2.900	–0.063
Bridge	1.175	*	179.7	2.947	–0.067
Hollow	1.175	*	179.9	3.147	–0.017
Ca-top	1.173	*	179.9	2.677	–0.064

In the initial structure, the C–O bond length of the CO_2 molecule is 1.177 Å and the ∠OCO angle is 179 °. It is found that the bond length and bond angle of CO_2 remained the same before and after optimization, and the corresponding adsorption energies are 0.067, 0.017, and 0.064 eV, respectively, indicating that the vertical adsorption of CO_2 on the CaO surface was weak physical adsorption[16, 19].

Fig. 2a is the initial structure before optimization. CO_2 is kept vertical at a position of 2.9 Å directly above the O ion on the CaO surface, and the corresponding adsorption energy is +0.02 eV. After adding van der Waals correction, the adsorption energy obtained is –0.06 eV, indicating a weak interaction between CO_2 molecule and CaO (100) surface[41].

Through adjusting the distance between CO_2 and the surface and several optimizations, the CO_2 molecule still had no change in bond length and bond angle. When CO_2 molecules are vertically adsorbed on the CaO (100) surface, CO_2 tends to stay away from the CaO surface. Therefore, the interaction between CO_2 and CaO surface mainly comes from the Van der Waals interaction.

3. 2 CO_2 adsorbed parallelly on the CaO(100) surface

As shown in Table 2, O-top site C–O_S bond length is 1.389 Å, indicating a partial double bond between

the C atom and O_S. The bridge site bond length is 1.407 Å, thereby slightly larger and corresponding to a single C–O bond. This value is similar to other existing theoretical calculations. For example, the bond length obtained by Schneider using a PW is 1.384 Å[18]. Pacchioni adopts the cluster model to obtain a bond length of 1.412 Å[14]. Sun et al. employ periodic structure to get a bond length of about 1.39～1.42 Å[36].

Compared with the gas phase CO_2 molecule, the C–O bond length was increased from 1.177 to 1.271 Å, revealing that the C–O bond is weakened after adsorption, and this value is close to the bond length of the carbonate. In the meantime, the bond angle also declined from the initial 179.9 °to 129.1 °, which is almost that of carbonate (120 °)[34]. As a consequence, CO_2 combines with oxygen ion on the surface of CaO at the O-top site to form a structure similar to CO_3^{2-}. Compared with the O-top site, the bridge site has a marginally larger C–O_S bond length of 1.407 Å. The C–O length and ∠OCO angle are slightly smaller, which are 1.264 Å and 127.9 °, respectively. The adsorption of CO_2 at the bridge site is unstable, and will eventually generate carbonates with the oxygen ions nearby. At the same time, C and oxygen atoms in CO_2 are in the same plane as the surface O_S, Ca_2 and Ca_4 ion.

For the hollow adsorption configuration, the E_a is –0.1324 eV, and the CO_2 molecule has no change in bond length, which is a physical adsorption. The adsorption energy of Ca-top site is greater than zero, indicating that the carbon atoms in the CO_2 molecule will not bond with the surface Ca ions, nor will physical adsorption occur at this site. As can be seen from Table 2, the E_a at the O-top site is –1.394 and –1.361 eV at the bridge site. It was experimentally found that the adsorption enthalpy varied within the range of 140～200 kJ/mol, close to the adsorption energy calculated in this paper. The E_a calculated by Jensen and Pacchioni using the cluster model is between –60 and –100 kJ/mol[16, 19]. And on that basis, Solis calculated the Ea of isolated CO_2 in a Ca_9O_9 cluster model of 3 × 3 × 1 as 151 kJ/mol by increasing the number of atoms in the model[42]. This result is similar to the adsorption energy (146 kJ/mol) calculated by using a supercell with periodic boundary conditions.

In this paper, our simulation is based on the perfect CaO crystal, and the adsorption energy has certain differences compared with the calculated value because of some differences between the model structure used in our calculation and the limestone in the experiment. In the process of CO_2 adsorption on the surface of CaO(100), the different coordination environments of oxygen ions on the surface of CaO contribute to different adsorption energies after CO_2 adsorption[36]. It can be inferred that the experimental reaction heat value of 140～200 kJ/mol is a result of the reactions in different chemical environments, as the structures in nature are more complex and uncontrolled. Through the above analysis of CO_2 parallel adsorption on the surface of CaO, we conclude that the shorter the C–O bond length, the stronger its bonding and the greater the adsorption energy.

The electron transfers were also calculated for comparison through Bader charge, as shown in Fig. 6. The negative charge of O_1 and O_2 increased from 7.05 to 7.22 e, and for O_S it decreased from 7.49 to 7.30 e. After the adsorption of CO_2 molecules on the surface of CaO, the negative charge is accumulated to the C atoms in CO_2 through the O_S ions on the surface of CaO and eventually flows to the O atoms of CO_2, leading to a reduction of CaO surface electrons. The total number of electrons transferred from the surface to the CO_2 molecules can be obtained from Table 2 as 0.44 |e|. The work function calculated after O-top adsorption was 4.28 eV, which was 0.32 eV higher than the clean CaO surface (3.96 eV). The work function of bridge site is 4.14 eV, less than the value of the work function of O-top. The work function is the lowest energy required for electrons to escape from a solid surface and can therefore be used as a criterion for surface stability. The larger the work function is, the greater the energy required for the electrons to escape from the surface will be. The work function calculation is consistent with the Bader analysis result, which proves that carbonates formed by bonding CO_2 with oxygen ion at the O-top are the most stable adsorption structures.

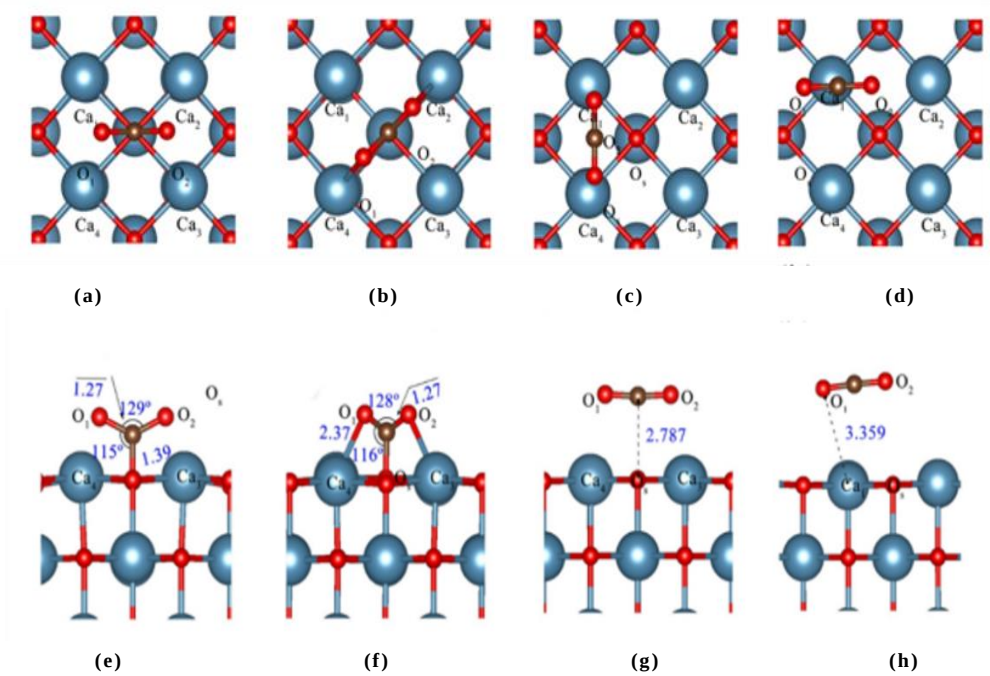

Fig. 4. Relaxed structures of CO_2 on CaO(100) in parallel. (a) and (b) Top and side views of CO_2 adsorbed on the O-top;(c) and (d) Top and side views of CO_2 adsorbed on the bridge site; (e) and (f) Top and side views of CO_2 adsorbed on the hollow; (g) and (h) Top and side views of CO_2 adsorbed on the Ca-top

Table 2. E_a and Geometric Properties of CO_2 Adsorbed Parallelly on the CaO Surface

Configuration	d(C–O) Å	d(C–O_S) Å	∠OCO (°)	E_a (eV)	qCO_2
O-top	1.271	1.389	129.1	–1.394	0.44
Bridge	1.264	1.407	127.9	–1.361	0.37
Hollow	1.179	*	177.8	–0.1324	0.01
Ca-top	1.179	*	177.7	+0.0612	0.00

3. 2. 1 Density of states

As calculated, no peak showed up on the clean surface of CaO in the range of –7～4 eV, but new peaks emerged in the valence band after CO_2 adsorption. This is attributed to the hybridization between the *p* orbital of the O_S atom on the CaO surface and the C atom orbital in CO_2, indicating a strong covalent interaction[41-43].

The delocalization of O^{2-} ion electrons on the surface of CaO moves toward the adsorbed CO_2 molecules, leading to the activation of the molecules[16]. The bending of CO_2 causes the $2\Pi_u$ orbital without electrons to split up into two symmetrical orbitals, $C_{2\infty}$, where one of the orbital energy is relatively lower, which enables the transfer of electrons from the surface to the CO_2 molecule in order to occupy the orbital[41].

The CO_2 molecule interacts with five-coordinated-O^{2-} on the surface of CaO (100). The $2p_z$ orbital of oxygen on the surface of CaO will overlap with the empty π^* MO orbital of CO_2 to form surface carbonate species[43]. When the negative charge moves from the surface to the CO_2 orbital, the C–O bond length of CO_2 likewise changes from 1.177 to 1.271 Å, and the transfer charge can be achieved from Bader charge.

In Fig. 5, the PDOS of carbon atom in CO_2 shows that the orbitals of the bridge are 0.282 eV higher in energy compared to the O-top species. This value, on one hand, can well explain the reasons for the difference of adsorption energy between the O-top bridge and bridge, and on the other hand, it indicates the bonding mechanism of these two configurations on the same level.

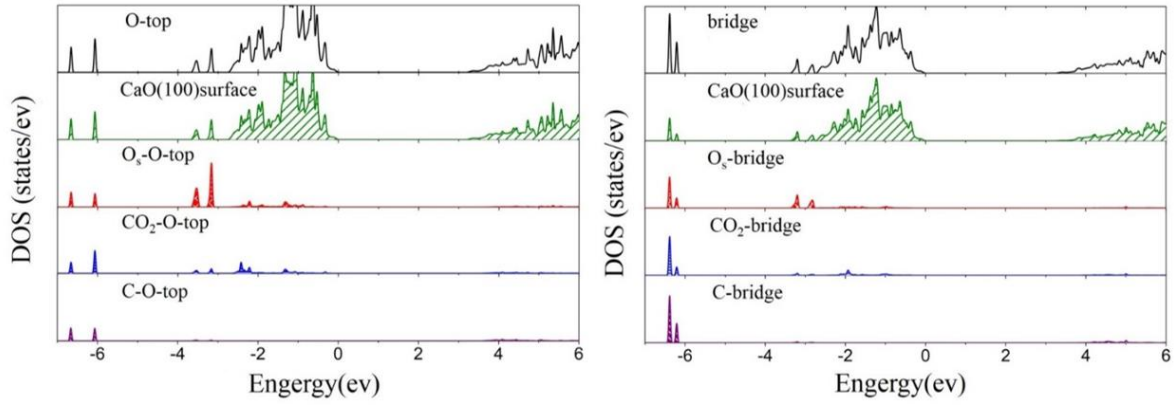

(a) **(b)**

Fig. 5. DOS of (a) Carbonate CO_3^{2-} on the O-top; (b) Carbonate CO_3^{2-} on the bridge

3. 2. 2 Differential charge density

As presented in Fig. 6, the bonding between O_S and C atoms is further confirmed by differential charge density. Yellow represents the electron-rich areas, whereas blue shows the electron-deficient areas[36,44-46]. The calculated differential charge density of CO_2 adsorption on the surface of CaO(100) demonstrates clearly the strong bonding among C–O and C–O_S ions, which is consistent with the CO_2 bonding in the bridge position. Thereby, the two configurations have comparable binding mechanisms.

By comparing the size of the yellow area around the O ion surface in Fig. 6, it can be seen that weak electron transport also happens among other atoms. The delocalized surface charge of calcium ions flows to the O ion. The positional charge transfer of O_S ions is considerably higher than that of the O^{2-} ions nearby.

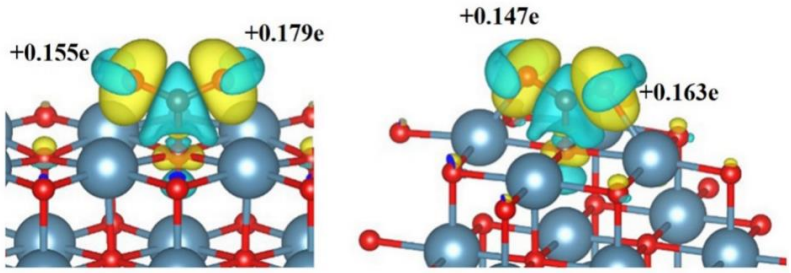

(a) **(b)**

Fig. 6. Charge density differences of CO_2 adsorption on the CaO(100) surface (isodensity plot 0.007 e/Å^3); (a) Carbonate CO_3^{2-} on the O-top; (b) Carbonate CO_3^{2-} on the bridge

3. 2. 3 Charge density analysis

To further study the bonding among O atoms in the O-top site CO_2 and Ca ions from the surface of CaO (100), further analysis has been performed on the charge density, as illustrated in Fig. 7. Fig. 7a displays the cross-section of the O-top charge density map along the surface of Ca_1, Ca_2, and O_S. Blue points out a decrease in charge density, whereas red signifies an increase in surface charge density. As a whole, the charge around the surface O increases while that around Ca decreases, which indicates that electrons migrate from Ca to O. In accordance with the contour line, the colour around O_S is darker, which demonstrates that after the negative charge is transferred from O_S to C, due to electronegativity, the O_S ion will attract more electrons from the surrounding coordinated Ca ions to supplement those electrons flowing to CO_2, thereby forming bluer regions in Fig. 7. Thus, O_S ions are bluer in Fig. 7.

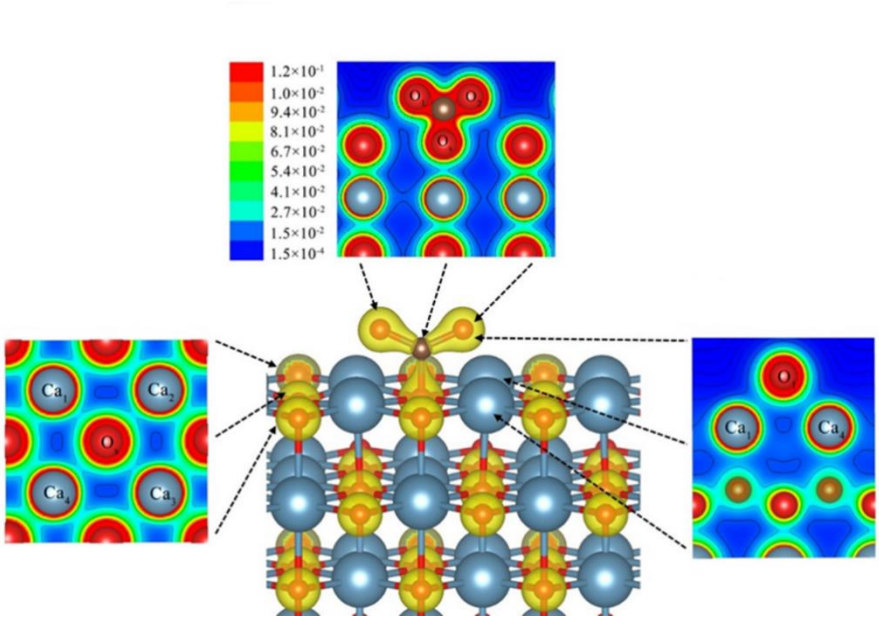

(a) (b) (c)

Fig. 7. Charge density distribution plots for (a) Surface of CaO (100); (b) CO_2 computed in the plane; (c) O_1, Ca_1 and Ca_4 plane

The VESTA software is utilized to measure the distance among O_S and the top four-coordinate Ca ions on the surface, finding that the bond length is around 2.52 Å, whereas the bond lengths among other oxygen ions and adjacent Ca^{2+} range from 2.29 to 2.34 Å. The bond length likewise confirmed that the bond between O_S–Ca is weaker. In Fig. 6, the charge density difference provides a similar outcome as the CO_2 conducted the Bader analysis, indicating that the surface Ca and O are bonded by an ionic bond.

Fig. 7b is a cross-sectional view of the charge density along the plane of the CO_2 molecule. It can be clearly observed that the charge density of CO_2 and surface O_S ions overlap with each other and undergo some deformation, highlighting that C–O and C–O_S bonds are covalent. The outcomes are consistent with those received from the PDOS analysis. Fig. 7c is a cross-sectional view of the charge density of the plane where the O_2 atoms in CO_2 and the surface Ca_2 and Ca_3 are located. It is evident from the figure that no bonding exists between O atoms and the surface Ca ions. According to the above analysis, the CO_2 bonding on the O-top site is quite obvious. CO_2 tends to bond with the surface oxygen ions to form a monodentate ligand.

Fig. 8 exhibits the corresponding charge density map of CO_2 adsorbed at the bridge site. Fig. 8a is a cross-sectional view of the charge density along the surface of CaO. We observed that the resulting charge density map was basically the same as shown in Fig. 5b. Compared with the electrons around other O ions, the electron around the O_S ion is substantially reduced.

Fig. 8b presents a cross-section view of the charge density along the plane of the CO_2 molecule, and it can be observed that the negative charge is transferred from Ca_1 to the O_1 atom. A similar situation likewise happens between Ca_2 and O_2, representing that the O atom in CO_2 is bound with the surface Ca ion through an ionic bond. O_1–Ca_1 and O_2–Ca_2 bond lengths are 2.371 and 2.372 Å, respectively, which are longer than the bulk O–Ca bond. Eventually, CO_2 generates carbonate with tridentate configuration with O ion by means of the bridge site, and CO_2 is in the same plane with the surface Ca_1, O_S, and Ca_2[47, 48].

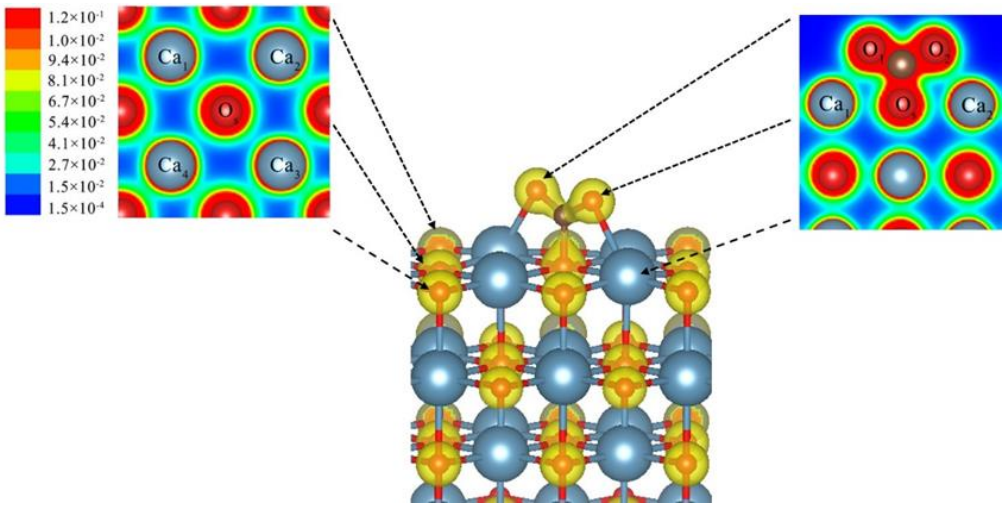

(a) **(b)**

Fig. 8. Charge density distribution plots for (a) Surface of CaO(100) and (b) Plane of the CO_2

Hence, based on the above analysis, the carbonate having monodentate configuration has a shorter C–O_S covalent bond compared with the tridentate carbonate. The binding energy released by the key formation is greater and the configuration is more stable. Nevertheless, tridentate carbonates will produce O–Ca ion bonds, thereby complementing the gap formed by covalent bonds. This is a reasonable explanation for the reason why the monodentate and tridentate configurations produced by CO_2 adsorption at the O-top position have a slight difference in adsorption energy.

4 CONCLUSION

We have studied the adsorption of CO_2 on the CaO(100) surface by density functional theory method. It was found that CO_2 tended to maintain linear adsorption on surface O atom through C atom, and no reaction occurred either via the O atom or at the Ca sites. We identified four different CO_2 adsorption configurations: O-top, bridge, hollow, and Ca-top. The most possible adsorption geometry is that carbon dioxide is adsorbed on the surface of calcium oxide in parallel with the adsorption angle to be 0 °. The monodentate ligand produced by adsorption has higher adsorption energy than the multidentate one. The results show that the adsorption energy changes with the change of C–O_S bond length. The shorter the C–O_S bond length, the greater the adsorption energy. This paper hopes to lay a foundation for subsequent research and provide a reliable theoretical basis for further experimental research and guidance for the industrial design and synthesis of new calcium oxide adsorbents.

REFERENCES

(1) Guiot, J.; Cramer, W. Climate change: the 2015 Paris agreement thresholds and Mediterranean basin ecosystems. *Science* **2016**, 354, 465–468.

(2) Wei, J.; Ge, Q.; Yao, R.; Wen, Z.; Fang, C.; Guo, L.; Xu, H.; Sun, J. Directly converting CO_2 into a gasoline fuel. *Nat. Commun*. **2017**, 8, 15174.

(3) Groenigen, K.; Qi, X.; Osenberg, C. W.; Luo, Y.; Hungate, B. A. Faster decomposition under increased atmospheric CO_2 limits soil carbon storage. *Science* **2014**, 344, 508–519.

(4) Michl, J. Photochemical CO_2 reduction: towards an artificial leaf. *Nat. Chem*. **2011**, 3, 268–269.

(5) Balaraman, E.; Gunanathan, C.; Zhang, J.; Shimon, L.; Milstein, D. Efficient hydrogenation of organic carbonates, carbamates and formates indicates alternative routes to methanol based on CO_2 and CO. *Nat. Chem*. **2011**, 3, 609–614.

(6) Richardson, R. D.; Holland, E. J.; Carpenter, B. K. A renewable amine for photochemical reduction of CO_2. *Nat. Chem*. **2011**,

3, 301−310.

(7) Meng, X.; Wang, T.; Liu, L.; Ouyang, S. X.; Ye, J. H. Photothermal conversion of CO_2 into CH_4 with H_2 over group VIII nanocatalysts: an alternative approach for solar fuel production. *Angew. Chem. Int. Ed*. **2014**, 126, 11478−11482.

(8) Chueh, W. C.; Falter, C.; Abbott, M.; Scipio, D.; Furler, P.; Haile, S. M.; Steinfeld, A. High-flux solar-driven thermochemical dissociation of CO_2 and H_2O using nonstoichiometric ceria. *Science* **2015**, 42, 1797−1801.

(9) Ahlers, S. J.; Bentrup, U.; Linke, D.; Kondratenko, E. V. An innovative approach for highly selective direct conversion of CO_2 into propanol using C_2H_4 and H_2. *Chemsuschem*. **2014**, 7, 2631−2639.

(10) Bi, Q. Y.; Lin, J. D.; Liu, Y. M.; Xie, S. H.; He, H. Y.; Cao, Y. Partially reduced iridium oxide clusters dispersed on titania as efficient catalysts for facile synthesis of dimethylformamide from CO_2, H_2 and dimethylamine. *Chem. Commun*. **2014**, 50, 9138−9140.

(11) Liu, X. H.; Ma, J. G.; Niu, Z.; Yang, G.; Cheng, P. An efficient nanoscale heterogeneous catalyst for the capture and conversion of carbon dioxide at ambient pressure. *Angew. Chem. Int. Ed*. **2015**, 54, 988−991.

(12) Angamuthu, R.; Byers, P.; Lutz, M.; Spek, A. L.; Bouwman, E. Electrocatalytic CO_2 conversion to oxalate by a copper complex. *Science* **2010**, 327, 313−315.

(13) Yaumi, A. L.; Bakar, M. Z.; Hameed, B. H. Recent advances in functionalized composite solid materials for carbon dioxide capture. *Energy* **2017**, 124, 461−480.

(14) Manovic, V.; Anthony, E. J. Thermal activation of CaO-based sorbent and self-reactivation during CO_2 capture looping cycles. *Environ. Sci. Technol*. **2008**, 42, 4170−4174.

(15) Eric, B.; Gontrand, L.; Cornelius, S. Corrigendum to: "the decrease of carbonation efficiency of CaO along calcination-carbonation cycles: experiments and modelling". *Chem. Eng. Sci*. **2010**, 64, 2136−2146.

(16) Pacchioni, G.; Ricart, J. M.; Illas, F. *Ab initio* cluster model calculations on the chemisorption of CO_2 and SO_2 probe molecules on MgO and CaO (100) surfaces. A theoretical measure of oxide basicity. *J. Am. Chem. Soc*. **1994**, 116, 10152−10158.

(17) Karlsen, E. J.; Nygren, M. A.; Pettersson, L. G. M. Comparative study on structures and energetics of NO_x, SO_x, and CO_x adsorption on alkaline-earth-metal oxides. *J. Phys. Chem. B* **2003**, 107, 7795−7802.

(18) Schneider, W. F. Qualitative differences in the adsorption chemistry of acidic (CO_2, SO_x) and amphiphilic (NOx) species on the alkaline earth oxides. *J. Phys. Chem. B* **2015**, 108, 273−282.

(19) Jensen, M. B.; Pettersson, L. G.; Swang, O.; Olsbye, U. CO_2 sorption on MgO and CaO surfaces: a comparative quantum chemical cluster study. *J. Phys. Chem. B* **2005**, 109, 16774−16781.

(20) And, E. K.; Burghaus, U. Adsorption kinetics and dynamics of CO, NO, and CO_2 on reduced CaO (100). *J. Phys. Chem. C* **2008**, 112, 7390−7400.

(21) Voigts, F.; Bebensee, F.; Dahle, S.; Volgmann, K.; Maus-Friedrichs, W. The adsorption of CO_2, and CO on Ca and CaO films studied with MIES, UPS and XPS. *Sur. Sci*. **2009**, 603, 40−49.

(22) Besson, R.; Vargas, M, R.; Favergeon, L. CO_2, adsorption on calcium oxide: an atomic-scale simulation study. *Sur. Sci*. **2012**, 606, 490−495.

(23) Zhang, Y.; Hu, J. M.; Cao, Q. Z.; Cao, Q. Z.; Qiu, M.; Yi, L.; Huang, X.; Zhang, Y. F. Density functional theory studies on the adsorption of CO_2 on different CaO surfaces. *Chin. J. Struct. Chem*. **2013**, 32, 1715−1723.

(24) Zhao, B. F.; Wang, J. W.; Zhu, D.; Song, G.; Yang, H. J.; Chen, L.; Sun, L. Z.; Yang, S. X.; Guan, H. B.; Xie, X. P. Adsorption characteristics of gas molecules (H_2O, CO_2, CO, CH_4, and H_2) on CaO-based catalysts during biomass thermal conversion with in situ CO_2 capture. *Catalysts* **2019**, 9, 757−766.

(25) Wang, W. J.; Fan, L. L.; Wang, G. P.; Li, Y. H. CO_2 and SO_2 sorption on the alkali metals doped CaO(100) surface: a DFT-D study. *Appl. Surf. Sci*. **2017**, 425, 972−977.

(26) Hammami, R.; Dhouib, A.; Fernandez, S.; Minot, C. CO_2 adsorption on (001) surfaces of metal monoxides with rock-salt structure. *Catal. Today* **2008**, 139, 227−233.

(27) Kresse, G.; Furthmüller, J. Efficiency of *ab-initio* total energy calculations for metals and semiconductors using a plane-wave basis set. *Comp. Mat. Sci*. **1996**, 6, 15−50.

(28) Kresse, G.; Joubert, D. From ultrasoft pseudopotentials to the projector augmented-wave method. *Phys. Rev. B* **1999**, 59, 1758−1775.

(29) Blöchl, P. E. Projector augmented-wave method. *Phys. Rev. B. Condens. Matter*. **1994**, 50, 17953−17979.

(30) Perdew, J. P.; Chevary, J. A.; Vosko, S. H.; Jackson, K. A.; Pederson, M. R.; Singh, D. J.; Fiolhais, C. Erratum: atoms, molecules, solids, and surfaces: applications of the generalized gradient approximation for exchange and correlation. *Phys. Rev. B. Condens. Matter*. **1993**, 46, 6671−6687.

(31) Skorodumova, N. V.; Hermansson, K.; Johansson, B. Structural and electronic properties of the (100) surface and bulk of alkaline-earth metal oxides. *Phys. Rev. B. Condens. Matter*. **2005**, 72, 1254141−1254147.

(32) Broqvist, P.; Grönbeck, H.; Panas, I. Surface properties of alkaline earth metal oxides. *Sur. Sci*. **2004**, 554, 262−271.

(33) Bajdich, M.; NØrskov, J. K.; Vojvodic, A. Surface energetics of alkaline-earth metal oxides: trends in stability and adsorption of small molecules. *Eprint. Arxiv*. **2015**, 91, 1−10.

(34) Cornu, D.; Guesmi, H.; Krafft, J. M.; Lauron-Pernot, H. Lewis acido-basic interactions between CO_2 and MgO surface: DFT and DRIFT approaches. *J. Phys. Chem. C* **2012**, 116, 6645−6654.

(35) Huygh, S.; Bogaerts, A.; Neyts, E. C. How oxygen vacancies activate CO_2 dissociation on TiO_2 anatase (001). *Conserv. Physiol*. **2015**, 3, 151−157.

(36) Sun, Z.; Wang, J.; Du, W.; Lu, G. M.; Li, P.; Song, X. F.; Yu, J. G. Density functional theory study on the thermodynamics and mechanism of carbon dioxide capture by CaO and CaO regeneration. *Rsc. Adv*. **2016**, 6, 39460−39468.

(37) Penninger, M. W.; Chang, H. K.; Thompson, L. T.; Schneider, W. F. DFT analysis of NO oxidation intermediates on undoped and doped $LaCoO_3$ perovskite. *J. Phys. Chem. C* **2015**, 119, 20488−20494.

(38) Momma, K.; Izumi, F. VESTA: a three-dimensional visualization system for electronic and structural analysis. *J. Appl. Crystallogr*. **2008**, 41, 653−658.

(39) Logsdail, A. J.; Mora-Fonz, D.; Catkiw, C. R. A.; Scanlon, D. O.; Sokol, A. A. Structural, energetic and electronic properties of (100) surfaces for alkaline earth metal oxides as calculated with hybrid density functional theory. *Sur. Sci*. **2015**, 642, 58−65.

(40) Liu, X.; Shi, J.; He, L.; Ma, X.; Xu, S. Modification of CaO-based sorbents prepared from calcium acetate for CO_2 capture at high temperature. *Chin. J. Chem. Eng*. **2016**, 25, 572−580.

(41) Hahn, K. R.; Iannuzzi, M.; Seitsonen, A. P.; Hutter, J. Coverage effect of the CO_2 adsorption mechanisms on CeO_2(111) by first principles analysis. *J. Phys. Chem. C* **2013**, 117, 1701−1711

(42) Solis, B. H.; Cui, Y.; Weng, X.; Seifert, J.; Freund, H. J. Initial stages of CO_2 adsorption on CaO: a combined experimental and computational study. *Phys. Chem. Chem. Phys*. **2017**, 19, 4231−4242.

(43) Tosoni, S.; Spinnato, D.; Pacchioni, G. DFT study of CO_2 activation on doped and ultrathin MgO films. *J. Phys. Chem. C* **2015**, 119, 27594−27602.

(44) Mishra, A. K.; Roldan, A.; Leeuw, N. H. CuO surfaces and CO_2 activation: a dispersion-corrected DFT+U study. *J. Phys. Chem. C* **2016**, 120, 2198−2214.

(45) Polfus, J. M.; Yildiz, B.; Tuller, H. L.; Bredesen, R. Adsorption of CO_2 and facile carbonate formation on $BaZrO_3$ surfaces. *J. Phys. Chem. C* **2018**, 122, 307−314.

(46) Hinojosa, J. A. Jr.; Antony, A.; Hakanoglu, C.; Asthagiri, A.; Weaver, J. F. Adsorption of CO_2 on a PdO (101) thin film. *J. Phys. Chem. C* **2012**, 116, 3007−3016.

(47) Downing, C. A; Sokol, A. A.; Catlow, C. R. The reactivity of CO_2 on the MgO (100) surface. *Phys. Chem. Chem. Phys*. **2013**, 16, 184−195.

(48) Preda, G.; Pacchioni, G.; Chiesa, M.; Giamello, E. Formation of CO_2-radical anions from CO_2 adsorption on an electron-rich MgO surface: a combined *ab initio* and pulse EPR study. *J. Phys. Chem. C* **2008**, 112, 19568−19576.